

## Performance of Commercial Alloys in Simulated Waste Incineration Environments

Brian A. Baker, Gaylord D. Smith and Lewis E. Shoemaker  
Special Metals Corporation  
3200 Riverside Drive  
Huntington, WV 25705-1771

### ABSTRACT

Commercial nickel-containing alloys have been exposed to simulated waste incineration conditions, comprising simulated flue gas and applied salt coatings, at 550° and 650°C using an inlet gas mixture comprised of N<sub>2</sub>-10% O<sub>2</sub>-10% CO<sub>2</sub>-20% H<sub>2</sub>O-1500ppm HCl-300ppm SO<sub>2</sub>. Samples were tested at 550° and 650°C after application of salt mixtures to the sample surface. The first salt mixture contained 20% ZnCl<sub>2</sub>, 40.9% PbCl<sub>2</sub>, 21.9% KCl, and 17.2% NaCl by weight while the second mixture contained 4.7% ZnCl<sub>2</sub>, 9.7% PbCl<sub>2</sub>, 2% KCl, 2.6% NaCl, 6.1% K<sub>2</sub>SO<sub>4</sub>, 4.9% Na<sub>2</sub>SO<sub>4</sub> and 70% Al<sub>2</sub>O<sub>3</sub> by weight. Testing at 650° was conducted with and without application of the first salt mixture to the surface. Testing at 550°C was conducted with application of each salt mixture, respectively. Corrosion performance has been evaluated metallographically and related to alloy composition using multiple regression analysis.

### INTRODUCTION

Utilization of waste incineration technology for disposal of municipal solid waste has become more prevalent in many countries. In locations where population densities are high, the use of landfills for waste disposal has become less feasible and waste incineration is a more attractive option. An additional advantage of incineration is the use of available heat for production of electricity. It is now known that chlorine-containing compounds are the primary corrosive species in waste incinerators, versus coal-fired boilers, where sulfur-containing compounds exacerbate corrosion.<sup>1</sup> Continued use of chlorinated plastic compounds and chloride salts such as NaCl by both industry and the general public

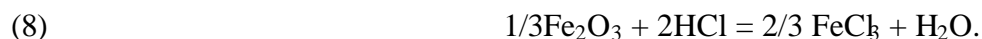
ensures the presence of appreciable HCl in the flue gas after combustion. The HCl in the flue gas becomes incorporated into chloride salts via reaction with alkali sulfates and oxides as well as surfaces of waterwall and superheater tubing. For example, consider reaction of sodium oxide with HCl to form NaCl and water:



Chlorides may then react with metal oxides and ultimately result in the release of chlorine<sup>2,3</sup>:



The liberated chlorine can then begin a self-sustaining cycle in the presence of oxygen through reaction with the metal surface, via the formation of and subsequent oxidation of,  $\text{FeCl}_2$  (or  $\text{FeCl}_3$  if HCl pressures are sufficiently high):



As shown in equation 8,  $\text{FeCl}_3$  can also possibly form through reaction of oxide scale with  $\text{FeCl}_2$ .<sup>4</sup> While sulfates are also present in waste incineration ash deposits, they are typically much lower in concentration than chlorides and are not thought to play a primary role in the corrosion mechanism taking place under the deposits. However, the presence of abundant  $\text{SO}_2$  in the flue gas could act to result in conversion of chlorides to sulfates:



This could potentially slow ultimate corrosion rates if the  $\text{SO}_2$ :HCl ratio in the flue gas is high enough. Krause's work has shown the effect of flue gas temperature and composition upon corrosion in waste incinerators.<sup>5</sup>

The common presence of heavy metals such as zinc and lead in the waste stream leads to the formation of low-melting and volatile chlorides. Table 1 shows melting and sublimation temperatures for metal chlorides and eutectics of metal chlorides as well as alkali sulfates. Figure 1 shows vapor pressure versus temperature for various metal chlorides. In addition to the composition of waste, increases in steam temperature in order to boost efficiency portend continued challenges for materials used to combat corrosion in waste incinerators.<sup>8</sup>

In addition to gaseous chloridation attack, severe corrosion attack can result from salt deposits which condense from the flue gas onto the metal surface. These deposits may be molten or partially fused, especially when heavy-metal chloride species are present, promoting dissolution of the metal

surface and dissolving protective oxides. Cathodic reduction of oxygen or steam would drive the anodic dissolution of the metal. Several electrochemical studies performed using chloride salt melts have shown that additions of molybdenum can suppress the corrosion rate; in addition, such studies have also shown nickel additions were considered to be favorable due to formation of NiO which is less soluble in a basic chloride salt melt than oxides of chromium.<sup>9,10,11</sup> Ishitsuka and Nose have recently shown that addition of MoO<sub>3</sub> to a synthetic waste incineration deposit has the effect of reducing the corrosion rate of 304 stainless steel partly by reducing the solubility of Cr<sub>2</sub>O<sub>3</sub>. Additions of tungsten or vanadium are expected to exert the same effect.<sup>9</sup> It would thus appear that alloying additions of nickel, chromium and molybdenum/tungsten may act synergistically to suppress the corrosion rate.

## EXPERIMENTAL

Testing was performed in a sealed electrically heated muffle furnace having a 100 mm diameter mullite tube. To form the test gas mixtures, oxygen and nitrogen were passed through a constant temperature water bath before the addition of CO<sub>2</sub>. The SO<sub>2</sub> and HCl test gases, pre-mixed with nitrogen, were then added to the gas stream. All flow rates were measured using electronic mass flow controllers. The flow of the gas mixtures was 250 cc/min. The chemical composition of the alloys tested is given in Table 2. Samples were taken from commercial plate and sheet and were exposed in the as-produced annealed condition. Surfaces were ground to a 120 grit finish prior to testing for samples obtained from thin sheet stock. Cylindrical samples were machined to a 32 micro-inch finish. Table 3 shows the inlet and predicted equilibrium percentages at 550°C and 650°C for the gas mixture used. Samples were exposed in the flowing gas with and without application of one of two chloride slurries. The compositions of the two mixtures are shown in Table 4. The slurry was prepared by first grinding the chloride salts into a fine powder using a mortar and pestle and then mixing with acetone. The slurry was then applied using a soft bristle brush. Mass gain resulting from application of the coating averaged 40 mg/cm<sup>2</sup>. Samples painted with the slurry were cycled at one week intervals during which loose scale was lightly removed mechanically and the slurry was re-applied. Samples were pushed into the hot zone of the furnace once the test atmosphere reached the desired temperature, using a sealed mechanism. The test gases flowed through a nickel oxide catalyst before reaching the samples to ensure equilibrium. Mass change results, measured and reported for samples exposed to simulated flue gas only at 650°C, were obtained after mechanical removal of the friable scale. Samples were prepared for depth of attack measurements by mounting in bakelite and polishing to a 0.05 μm alumina finish. Metal loss and depth of attack measurements were performed at 6 locations for each sample.

## RESULTS AND DISCUSSION

Table 5 and Figure 2 show metal loss and maximum attack results obtained after exposure of numerous alloys in N<sub>2</sub>-10% O<sub>2</sub>-10% CO<sub>2</sub>-20% H<sub>2</sub>O-1500ppm HCl-300ppm SO<sub>2</sub> at 650°C for 336 hours (i.e. two cycles). Samples were painted with chloride salt mixture 1. Duplicate samples were tested. Multiple linear regression of the attack rate versus levels of Ni, Cr, Mo and W for the alloys tested indicated that the attack rate was best correlated with the summation of %Ni + 2(%Cr + %Mo + %W); see Figure 3. Figures 4 and 5 show photomicrographs of alloys 625, 686, 600 and 825 after testing. Alloys 600 and 825 exhibited an extensive 'spongy' layer of oxide while alloys 625 and 686 showed a more distinct metal-to-scale boundary. Figure 6 shows mass change results after exposure for 336 hours in N<sub>2</sub>-10% O<sub>2</sub>-10% CO<sub>2</sub>-20% H<sub>2</sub>O-1500ppm HCl-300ppm SO<sub>2</sub> at 650°C without application of the chloride salt coating. In comparison with Table 5 and Figure 2, these results illustrate the accelerating effect that the salt coating had upon the corrosion rate.

Table 6 and Figure 7 show metal loss and maximum attack results obtained after exposure of numerous alloys in N<sub>2</sub>-10%O<sub>2</sub>-10%CO<sub>2</sub>-20%H<sub>2</sub>O-1500ppm HCl-300ppm SO<sub>2</sub> at 550°C for 336 hours, with samples painted with chloride salt mixture 1. Duplicate samples were tested. Multiple linear regression of attack rate versus levels of Ni, Cr, Mo, and W was performed for the alloys tested. These results indicated that the attack rate was best correlated with the summation of %Cr + 2(%Mo) + %W (Figure 8). Niobium was not incorporated into the analysis since alloy 625 was the only niobium-containing alloy tested and regression results including niobium indicated very high standard error. Comparing the results with those obtained at 650°C, using the same inlet gas and applied salt, some trends were noted. The iron-base alloys 825 and 803 showed a significant reduction in attack rate at the lower temperature, while the Ni-Cr-Fe alloys 600 and 690 experienced a fairly similar attack rate at both temperatures. The Ni-Cr-Mo alloys experienced slightly lower attack rates at 550°C. Figures 9 through 12 show photomicrographs of alloys 690, 825, 686 and 625 after testing. Extensive internal oxide formation is evident in the alloy 690 sample.

Figure 13 shows the results of four additional test exposures performed in N<sub>2</sub>-10%O<sub>2</sub>-10%CO<sub>2</sub>-20%H<sub>2</sub>O-1500ppm HCl-300ppm SO<sub>2</sub> at 550°C for 336 hours with salt mixture one applied to the surface, comparing alloys 625, 622 and C-22. Selection of alloys for this test series was driven by the interest of industry in this particular alloy group. Each data point shown represents the average of results obtained for two samples. With the exception of test exposure one, alloy 622 exhibited significant improvement over alloy 625. Applying the summation obtained using results from the earlier test under the same conditions at 650°C [%Cr + 2(%Mo) + %W] yields a total of 51 for alloy 622 and 39.5 for alloy 625. This treatment does not incorporate the effect of niobium. Experimental results reported by Nylöf and Häggblom indicated no effect of niobium in developmental 625-type alloys having varied levels of Ni, Cr, Fe, and Nb.<sup>12</sup> Figure 14 shows the results of exposure under the same conditions at 550°C of samples machined from submerged-arc weldments made onto steel. Spectrographic analysis of both the top and backsides of the sample indicated similar iron contents throughout the removed sample. Each data point shown represents the average of results for two samples. Figure 15 shows a schematic of the sample configuration. The iron content of the alloy 625 weld overlay sample was determined to be 14.5%; the alloy 622 weld overlay sample iron content was 12.3%. The results indicate that the attack rates were only slightly higher for the weld overlay samples, in comparison with wrought samples. In addition, the corrosion rate for the alloy 625 samples was also slightly higher than that of the alloy 622 samples, confirming the results obtained using wrought samples.

Figure 16 shows results obtained after testing in N<sub>2</sub>-10%O<sub>2</sub>-10%CO<sub>2</sub>-20%H<sub>2</sub>O-1500ppm HCl-300ppm SO<sub>2</sub> at 550°C for 336 hours with salt mixture two (9.7% PbCl<sub>2</sub>-4.7% ZnCl<sub>2</sub>-2% KCl-2.6% NaCl-6% K<sub>2</sub>SO<sub>4</sub>-4.9% Na<sub>2</sub>SO<sub>4</sub>-70% Al<sub>2</sub>O<sub>3</sub> by weight; equimolar amounts of each salt) applied to the sample surface. Duplicate samples were tested. The results indicate a change in the corrosion mechanism, from chloridation to sulfidation, with alloy 690 and the iron-base alloys exhibiting the best performance. Evaluation of sample microstructures indicated the presence of sulfides. The heavy metal chlorides may have volatilized rapidly (Figure 1), leaving fairly low levels of KCl and NaCl behind (2.8% and 3.6% by weight after normalizing in the absence of the heavy metal chlorides). The higher melting points of the alkali sulfates, most notably K<sub>2</sub>SO<sub>4</sub> which is more abundant in salt mixture two, and the lower level of chloride present in salt mixture two may account for the observed corrosion response.

## CONCLUSIONS

Testing of several nickel-containing alloys has been performed in N<sub>2</sub>-10%O<sub>2</sub>-10%CO<sub>2</sub>-20%H<sub>2</sub>O-1500ppm HCl-300ppm SO<sub>2</sub> at 550°C and 650°C for 336 hours with a salt mixture comprised of 20%

ZnCl<sub>2</sub>, 40.9% PbCl<sub>2</sub>, 21.9% KCl, and 17.2% NaCl (by weight) applied to the sample surface. Multiple linear regression correlating attack rate with levels of Ni, Cr, Mo and W was performed. Regression results indicate that attack rate at 550°C was best-correlated with the summation of %Cr + 2(%Mo) + %W; the attack rate at 650°C was best correlated with the summation of %Ni + 2(%Cr + %Mo + %W). Increasing temperature caused dramatic increase in the attack rate of the iron-base alloys tested. Testing for 336 hours at 650°C in N<sub>2</sub>-10%O<sub>2</sub>-10%CO<sub>2</sub>-20%H<sub>2</sub>O-1500ppm HCl-300ppm SO<sub>2</sub> with no applied salt resulted in only minimal attack as indicated by low mass gain for all samples tested.

Testing has also been performed in N<sub>2</sub>-10%O<sub>2</sub>-10%CO<sub>2</sub>-20%H<sub>2</sub>O-1500ppm HCl-300ppm SO<sub>2</sub> at 550°C for 336 hours with a mixture comprised of 9.7% PbCl<sub>2</sub>, 4.7% ZnCl<sub>2</sub>, 2% KCl, 2.6% NaCl, 6% K<sub>2</sub>SO<sub>4</sub>, 4.9% Na<sub>2</sub>SO<sub>4</sub>, and 70% Al<sub>2</sub>O<sub>3</sub> by weight, applied to the sample surface. This exposure resulted in sulfidation attack, and the best performance was exhibited by alloy 690, followed by the iron-base alloys 803 and 825.

## REFERENCES

1. G. Sorell, "The Role of Chlorine in High Temperature Corrosion in Waste-to-Energy Plants," *Materials at High Temperatures*, 14 (3), 1997, pp. 207-220.
2. F. Soutrel, C. Rapin, P. Steinmetz, and G. Pierotti, "Corrosion of Fe, Ni, and Cr and Their Alloys in Simulated Municipal Waste Incinerator Conditions," *CORROSION/98*, Paper No. 428, NACE International, 1998.
3. H. J. Grabke, E. Reese, and M. Spiegel, "The Effects of Chlorides, Hydrogen Chloride, and Sulfur Dioxide in the Oxidation of Steels Below Deposits," *Corrosion Science*, 37 (3), 1995, pp. 1023-1043.
4. I. G. Wright, V. Nagarajan, and H. H. Krause, "Mechanisms and Fireside Corrosion by Chlorine and Sulfur in Refuse-Firing," *CORROSION/93*, Paper No. 201, NACE International, 1993.
5. H. H. Krause, "Effects of Flue-Gas Temperature and Composition on Corrosion from Refuse Firing," *CORROSION/91*, Paper No. 242, NACE International, 1991.
6. I. G. Wright, H. H. Krause, and R. B. Dooley, "A Review of Materials Problems and Solutions in U.S. Waste-Fired Steam Boilers," *CORROSION/95*, Paper No. 562, NACE International, 1995.
7. "Smithells Metals Reference Book, E. A. Brandes and G. B. Brook, Eds., Butterworth-Heinemann, 1998.
8. Y. Kawahara, et al., "Demonstration of New Corrosion-Resistant Superheater Tubings in a High-Efficiency Waste-to-Energy Plant," *CORROSION/2000*, Paper No. 265, NACE International, 2000.
9. A. Nishitaka and S. Haruyama, "Electrochemical Monitoring of the Corrosion of Ni, Fe, and Their Alloys in Molten Salts," *Corrosion*, 42 (10), 1986, pp. 578-584.
10. K. Nakagawa, Y. Matsunaga, and K. Yukawa, "An Electrochemical Investigation of Corrosion of Superheater Tube in Waste Incineration Environment," *CORROSION/97*, Paper No. 164, NACE International, 1997.
11. Ishitsuka T. and K. Nose, "Solubility Study on Protective Oxide Films in Molten Chlorides Created by Refuse Incineration Environment," *Materials and Corrosion*, 51, 2000, pp. 177-181.
12. L. Nylöf and E. Häggblom, "Corrosion of Experimental Superheater Alloys in Waste Fuel Combustion," *CORROSION/97*, Paper No. 154, NACE International, 1997.

Table 1. Melting and Sublimation Temperatures for Metal Chlorides, Eutectic Mixtures of Metal Chlorides and Alkali Sulfates<sup>6,7</sup>

Eutectic Mixture, Mole %	Melting Point	Sublimation Point
	°C	°C
SnCl <sub>2</sub>	247	652
FeCl <sub>3</sub>	304	315
25 NaCl-75 FeCl <sub>3</sub>	156	n/a
ZnCl <sub>2</sub>	318	732
37 PbCl <sub>2</sub> -63 FeCl <sub>3</sub>	175	n/a
60 SnCl <sub>2</sub> -40 KCl	176	n/a
70 SnCl <sub>2</sub> -30 NaCl	183	n/a
70 ZnCl <sub>2</sub> -30 FeCl <sub>3</sub>	200	n/a
20 ZnCl <sub>2</sub> -80 SnCl <sub>2</sub>	204	n/a
55 ZnCl <sub>2</sub> -45 KCl	230	n/a
PbCl <sub>2</sub>	498	954
70 ZnCl <sub>2</sub> -30 NaCl	262	n/a
60 KCl-40 FeCl <sub>2</sub>	355	n/a
58 NaCl-42 FeCl <sub>2</sub>	370	n/a
70 PbCl <sub>2</sub> -30 NaCl	410	n/a
52 PbCl <sub>2</sub> – 48 KCl	411	n/a
72 PbCl <sub>2</sub> -28 FeCl <sub>2</sub>	421	n/a
90 PbCl <sub>2</sub> -10 MgCl <sub>2</sub>	460	n/a
80 PbCl <sub>2</sub> -20 CaCl <sub>2</sub>	475	n/a
49 NaCl-51 CaCl <sub>2</sub>	500	n/a
KCl	772	1407
NaCl	801	1465
Na <sub>2</sub> SO <sub>4</sub>	885	n/a
K <sub>2</sub> SO <sub>4</sub>	1069	n/a

Table 2. Chemical Composition of Alloys Examined in this Study

Alloy	Fe	Ni	Cr	Mo	Al	Ti	Si	Mn	C	Others
803	38	35	26	-	0.4	0.4	0.8	0.8	0.08	-
890	29	41	25	1.5	0.3	0.3	1.5	.8	0.08	.4 Nb, 0.25Ta
825	27	43	21.5	3.0	0.1	0.9	0.2	0.5	0.03	1.6 Cu
FM72	0.3	56	43	-	0.1	0.6	-	-	0.01	-
C-276	5.5	57	15.5	16	0.1	0.2	-	-	-	3.8 W
622	2.5	57	20	14	0.2	-	-	0.2	0.01	3.0 W
C-22	3.0	56	22	13	-	-	0.2	-	0.02	3.0 W
686/686CPT	-	58	20	16	0.2	0.2	0.02	0.2	0.01	3.8 W
C-2000	-	59	23	16	-	-	0.08	-	0.01	1.6 Cu
625	2.5	61	21.5	9.0	0.1	0.2	0.2	0.2	0.05	3.6 Nb
690	9	61.5	29	-	0.1	0.2	-	-	0.03	-
600	8	74	15.5	-	-	-	0.2	0.2	0.04	-

Table 3. Inlet and Equilibrium Composition for Simulated Waste Incineration Flue Gas Mixture

Gas Condition	Gas Composition (Volume %, Unless Noted, Excess is Nitrogen)						
	HCl	Cl <sub>2</sub>	SO <sub>2</sub>	SO <sub>3</sub>	O <sub>2</sub>	H <sub>2</sub> O	CO <sub>2</sub>
Inlet	1500 ppm	---	300 ppm	---	10	20	10
Equilibrium, 550°C	1492 ppm	0.0006	36 ppm	0.0265	10.015	20.057	10.028
Equilibrium, 650°C	1499 ppm	0.0002	118 ppm	0.0183	10.019	20.056	10.028

Table 4. Salt Mixture Compositions

	Salt 1 <sup>a</sup>	Salt 2 <sup>b</sup>
	Weight %	Weight %
PbCl <sub>2</sub>	40.9	9.7
ZnCl <sub>2</sub>	20.0	4.7
KCl	21.9	2.0
NaCl	17.2	2.6
K <sub>2</sub> SO <sub>4</sub>	---	6.1
Na <sub>2</sub> SO <sub>4</sub>	---	4.9
Al <sub>2</sub> O <sub>3</sub>	---	70

a - Wt. % Cl = 41.7

b - Wt. % Cl = 24.6; Wt. % S = 7.4

Table 5. Corrosion Rate Measurements after Exposure for 336 Hours in N<sub>2</sub>-10%O<sub>2</sub>-10%CO<sub>2</sub>-20%H<sub>2</sub>O-1500ppm HCl-300 ppm SO<sub>2</sub> at 650°C - Samples Painted with Ash 1

Alloy	Metal Loss		Maximum Attack		Metal Loss Rate		Maximum Attack Rate	
	Inches	mm	Inches	mm	mpy	mm/yr	mpy	mm/yr
625	0.0033	0.08	0.0033	0.08	86.0	2.2	86.0	2.2
625	0.0031	0.08	0.0036	0.09	80.8	2.1	92.6	2.4
686	0.0032	0.08	0.0035	0.09	83.4	2.1	89.9	2.3
686	0.0045	0.11	0.0045	0.11	117.3	3.0	117.3	3.0
C-276	0.0054	0.14	0.0054	0.14	139.5	3.5	139.5	3.5
C-276	0.0059	0.15	0.0059	0.15	153.8	3.9	153.8	3.9
C-2000	0.0064	0.16	0.0064	0.16	166.9	4.2	166.9	4.2
C-2000	0.0120	0.30	0.0120	0.30	311.6	7.9	311.6	7.9
600	0.0054	0.14	0.0187	0.47	139.5	3.5	487.5	12.4
600	0.0244	0.62	0.0244	0.62	634.8	16.1	634.8	16.1
690	0.0112	0.28	0.0126	0.32	292.0	7.4	328.5	8.3
690	0.0153	0.39	0.0153	0.39	398.9	10.1	398.9	10.1
890	0.0192	0.49	0.0192	0.49	499.3	12.7	499.3	12.7
890	0.0313	0.80	0.0313	0.80	816.0	20.7	816.0	20.7
803	0.0251	0.64	0.0251	0.64	653.1	16.6	653.1	16.6
803	0.0323	0.82	0.0323	0.82	842.1	21.4	842.1	21.4
825	0.0310	0.79	0.0310	0.79	806.9	20.5	806.9	20.5
825	0.0394	1.00	0.0394	1.00	1025.9	26.1	1025.9	26.1

Table 6. Corrosion Rate Measurements after Exposure for 336 Hours in N<sub>2</sub>-10%O<sub>2</sub>-10%CO<sub>2</sub>-20%H<sub>2</sub>O-1500ppm HCl-300 ppm SO<sub>2</sub> at 550°C - Samples Painted with Ash 1

Alloy	Metal Loss		Maximum Attack		Metal Loss Rate		Maximum Attack Rate	
	Inches	mm	Inches	mm	mpy	mm/yr	mpy	mm/yr
686CPT	0.0018	0.05	0.0022	0.06	46.9	1.2	57.4	1.5
FM72	0.0033	0.08	0.0041	0.10	86.0	2.2	106.9	2.7
C-276	0.0027	0.07	0.0028	0.07	70.4	1.8	73.0	1.9
C-276	0.0033	0.08	0.0037	0.09	86.0	2.2	95.2	2.4
686	0.0043	0.11	0.0043	0.11	112.1	2.8	112.1	2.8
686	0.0051	0.13	0.0051	0.13	131.7	3.3	131.7	3.3
625	0.0047	0.12	0.0047	0.12	122.5	3.1	122.5	3.1
625	0.0056	0.14	0.0057	0.14	146.0	3.7	147.3	3.7
C-2000	0.0058	0.15	0.0059	0.15	151.2	3.8	152.5	3.9
C-2000	0.0056	0.14	0.0068	0.17	146.0	3.7	177.3	4.5
825	0.0076	0.19	0.0076	0.19	198.1	5.0	198.1	5.0
825	0.0104	0.26	0.0104	0.26	269.8	6.9	269.8	6.9
803	0.0068	0.17	0.0091	0.23	177.3	4.5	235.9	6.0
803	0.0125	0.32	0.0142	0.36	324.6	8.2	370.2	9.4
690	0.0172	0.44	0.0172	0.44	448.4	11.4	448.4	11.4
690	0.0153	0.39	0.0177	0.45	398.9	10.1	460.2	11.7
600	0.0133	0.34	0.0133	0.34	345.4	8.8	345.4	8.8
600	0.0252	0.64	0.0252	0.64	657.0	16.7	657.0	16.7

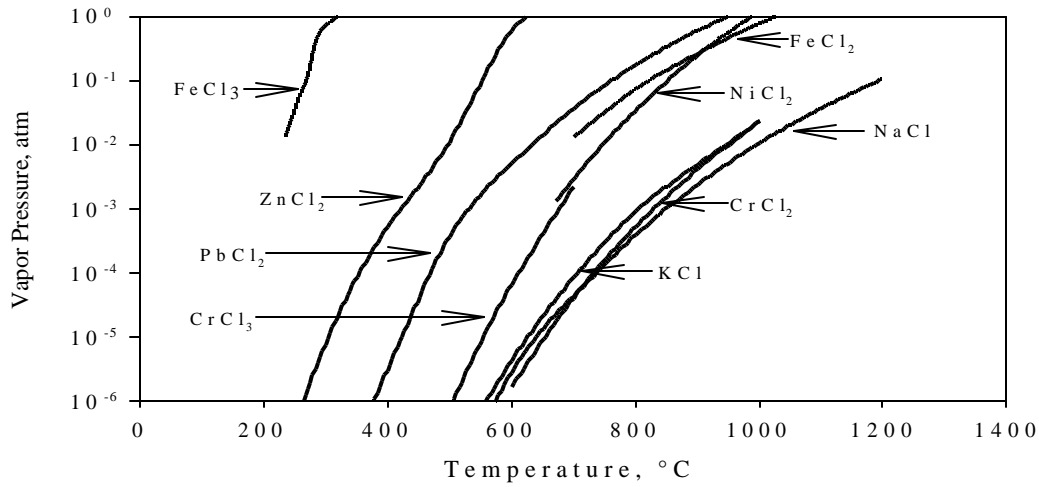


Figure 1. Dependence of vapor pressure upon gas temperature for selected chloride species.<sup>7</sup>

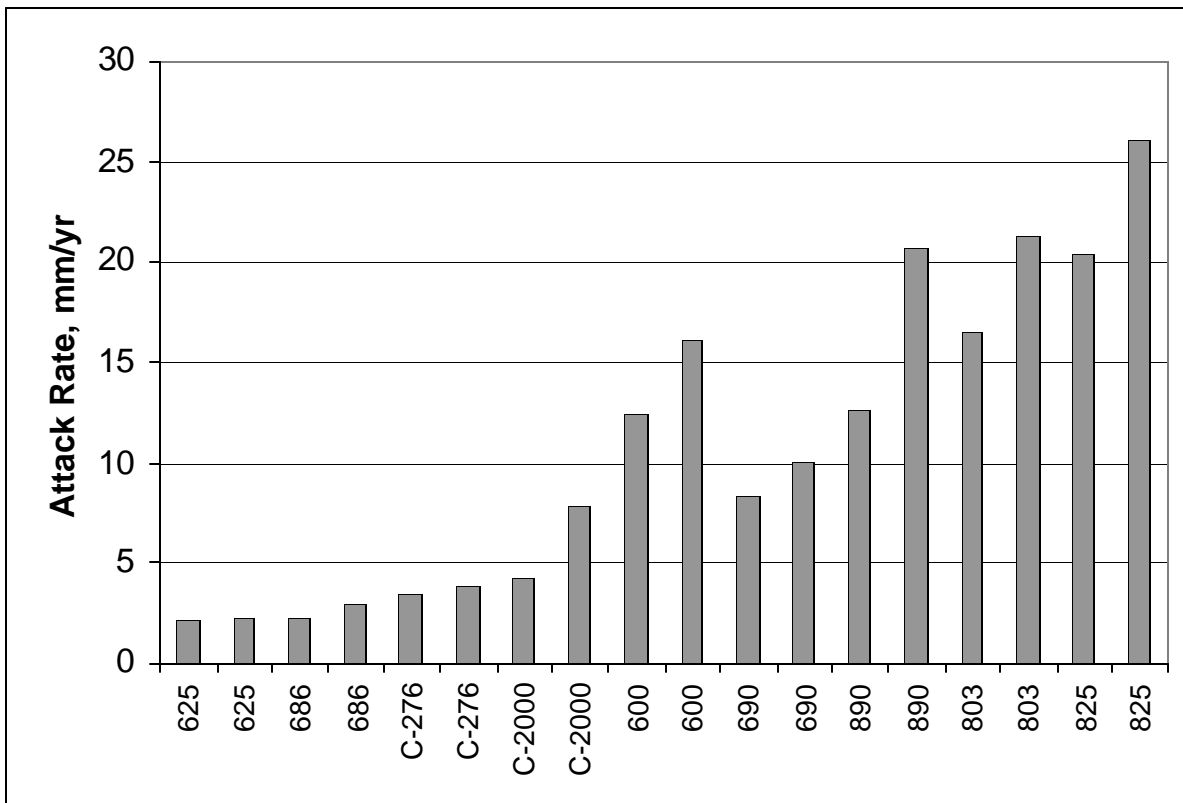


Figure 2. Corrosion rate measurements after exposure for 336 hours in N<sub>2</sub>-10%O<sub>2</sub>-10%CO<sub>2</sub>-20%H<sub>2</sub>O-1500ppm-HCl-300 ppm SO<sub>2</sub> at 650°C. Samples were painted with salt mixture 1.

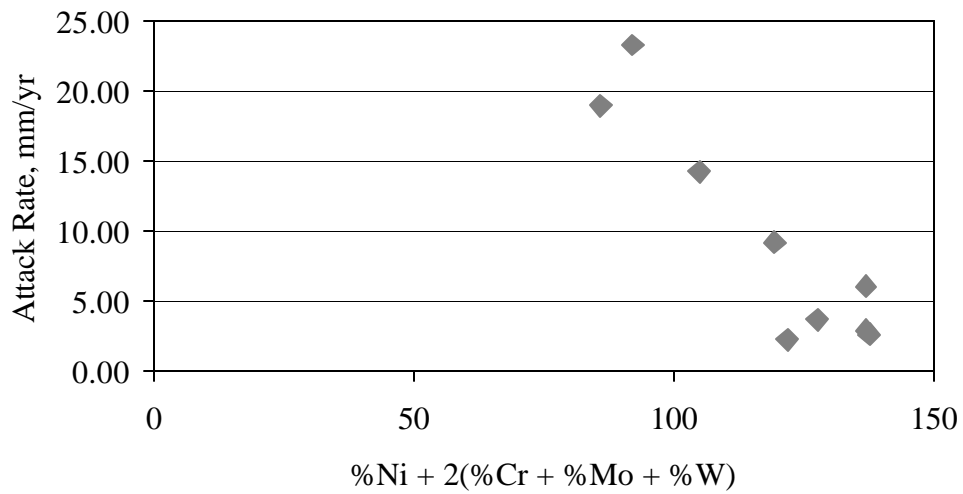


Figure 3. Corrosion rate versus composition after exposure for 336 Hours in N<sub>2</sub>-10%O<sub>2</sub>-10%CO<sub>2</sub>-20% H<sub>2</sub>O-1500ppm HCl-300ppm SO<sub>2</sub> at 650°C. Samples were painted with salt mixture 1.

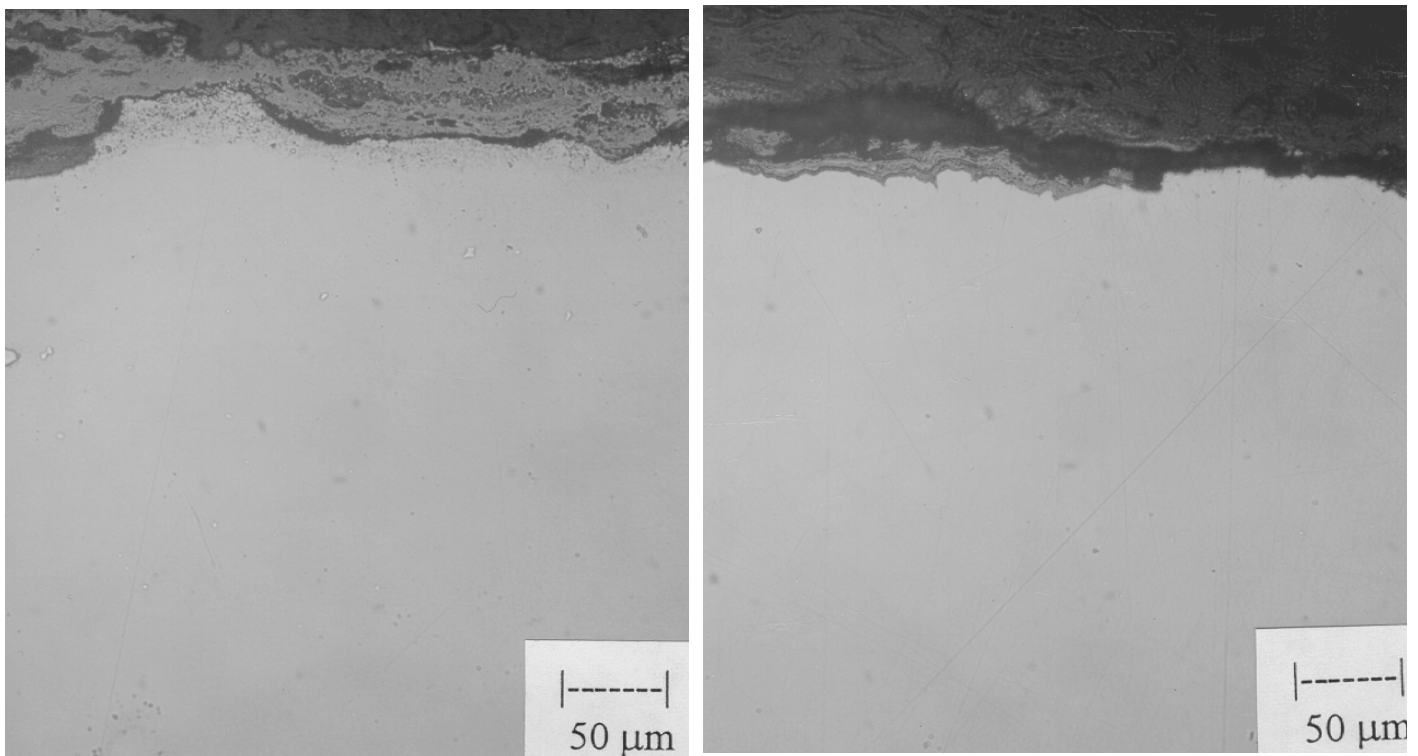


Figure 4. Photomicrographs showing cross sections of alloys 625 (left) and 686 (right) after exposure in N<sub>2</sub>-10%O<sub>2</sub>-10%CO<sub>2</sub>-20%H<sub>2</sub>O-1500ppm HCl-300ppm SO<sub>2</sub> at 650°C. Samples were coated with salt mixture 1. Unetched.

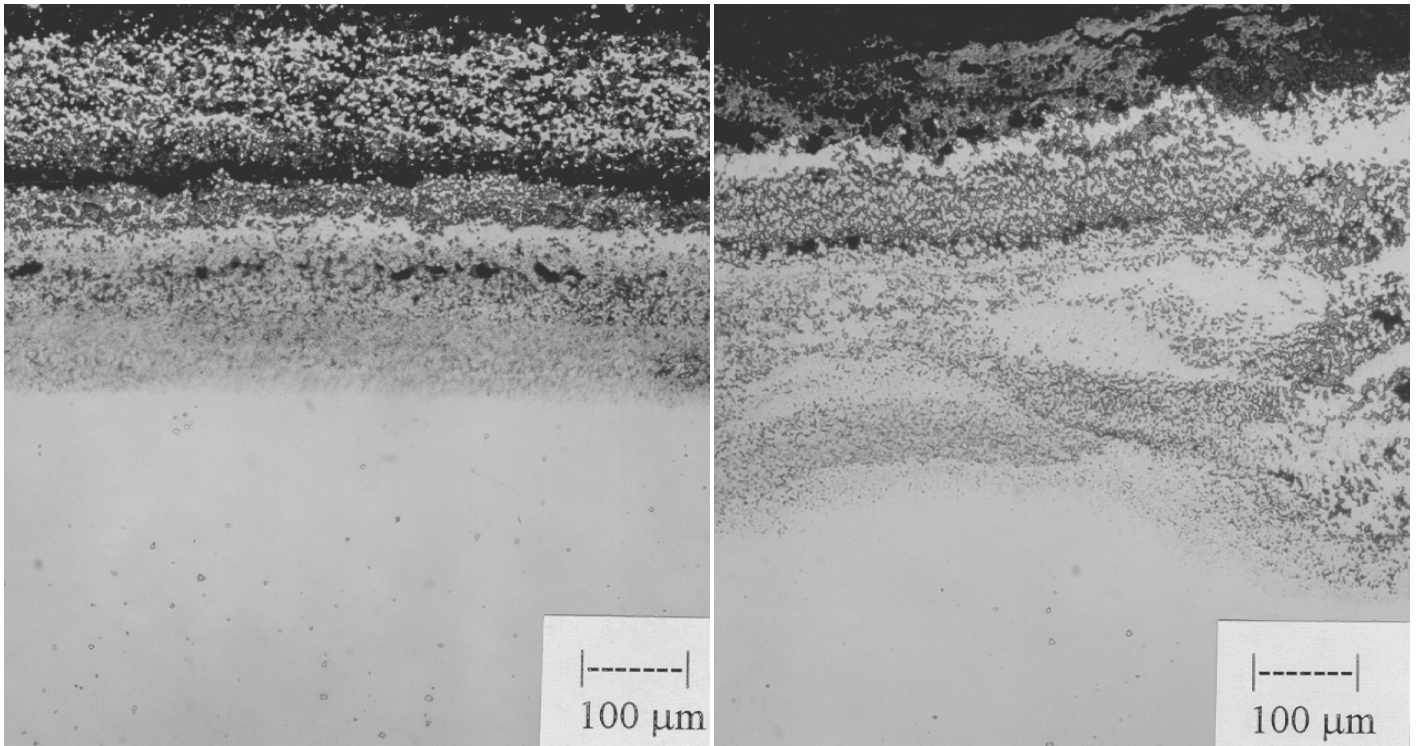


Figure 5. Photomicrographs showing cross sections of alloys 600 (left) and 825 (right) after exposure in  $N_2$ -10% $O_2$ -10% $CO_2$ -20% $H_2O$ -1500ppm HCl-300ppm  $SO_2$  at 650°C. Samples were coated with salt mixture 1. Unetched

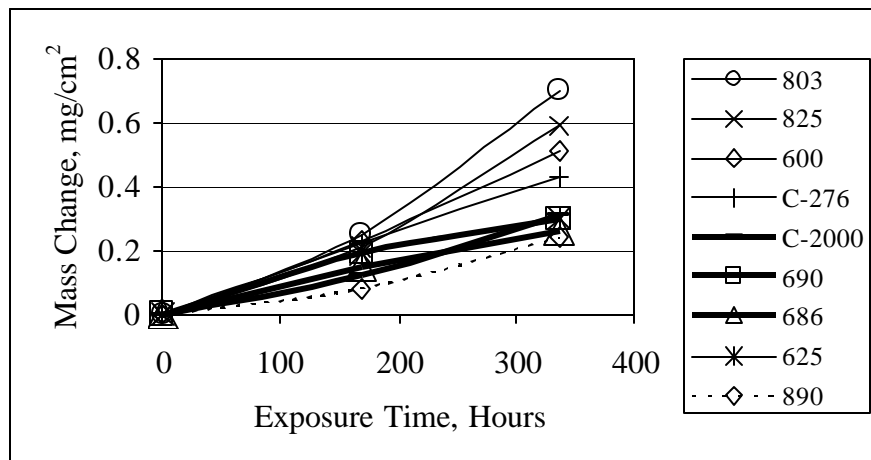


Figure 6. Mass change measurements after exposure for 336 hours in  $N_2$ -10% $O_2$ -10% $CO_2$ -20% $H_2O$ -1500ppm HCl-300ppm  $SO_2$  at 650°C. Samples were not painted with salt mixture.

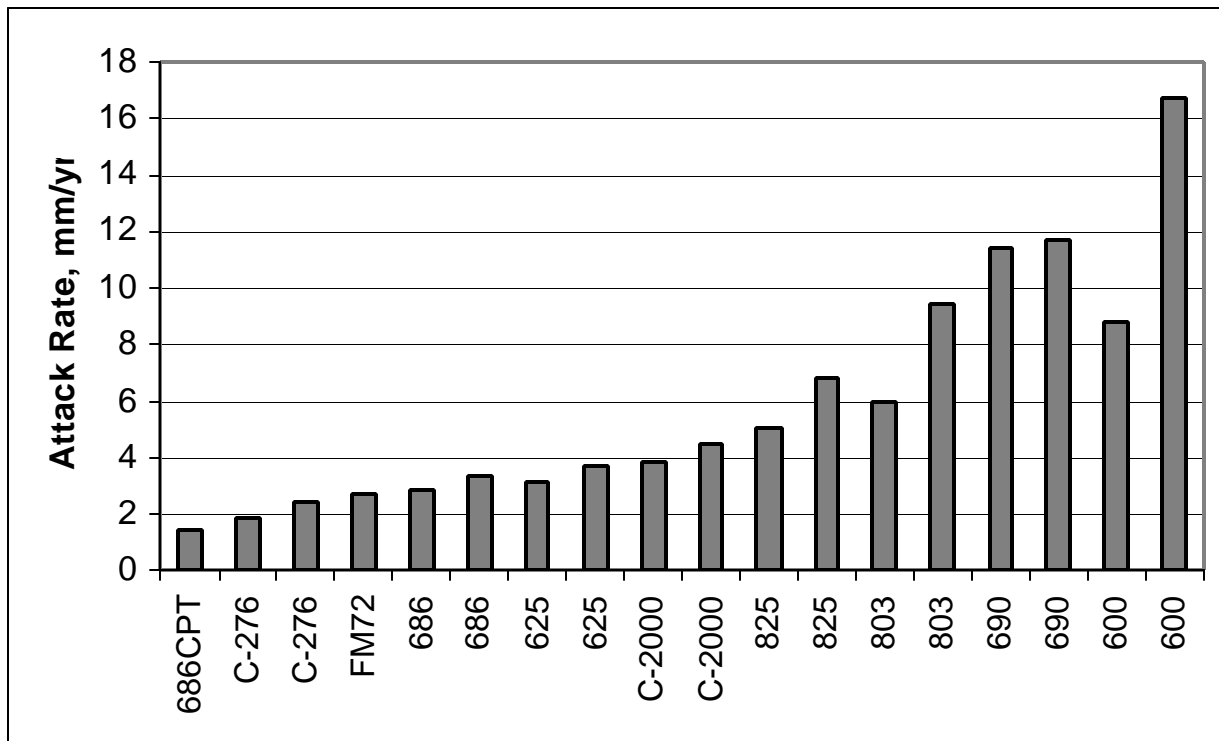


Figure 7. Corrosion rate measurements after exposure for 336 hours in  $N_2$ -10% $O_2$ -10% $CO_2$ -20% $H_2O$ -1500ppm HCl-300ppm  $SO_2$  at 550°C. Samples were painted with salt mixture 1.

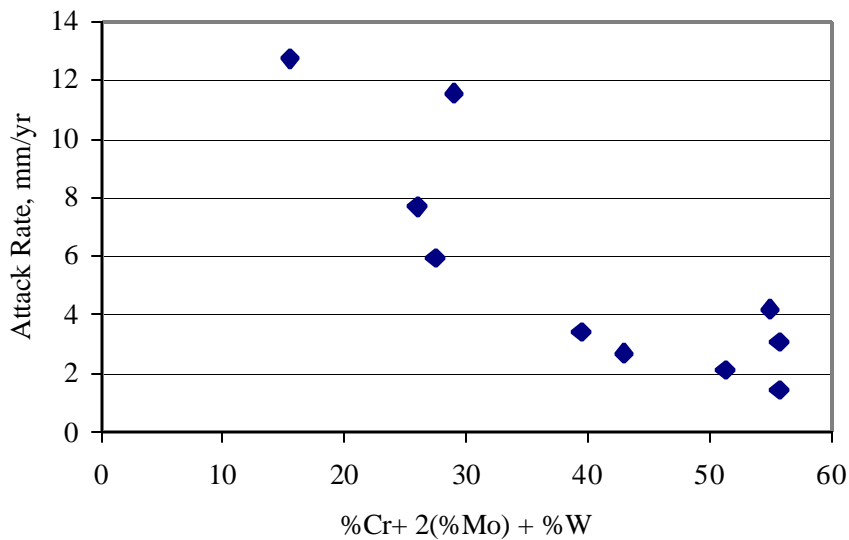


Figure 8. Corrosion rate measurements versus composition after exposure for 336 Hours in  $N_2$ -10% $O_2$ -10% $CO_2$ -20% $H_2O$ -1500ppm HCl-300 ppm  $SO_2$  at 550°C. Samples were painted with salt mixture 1.

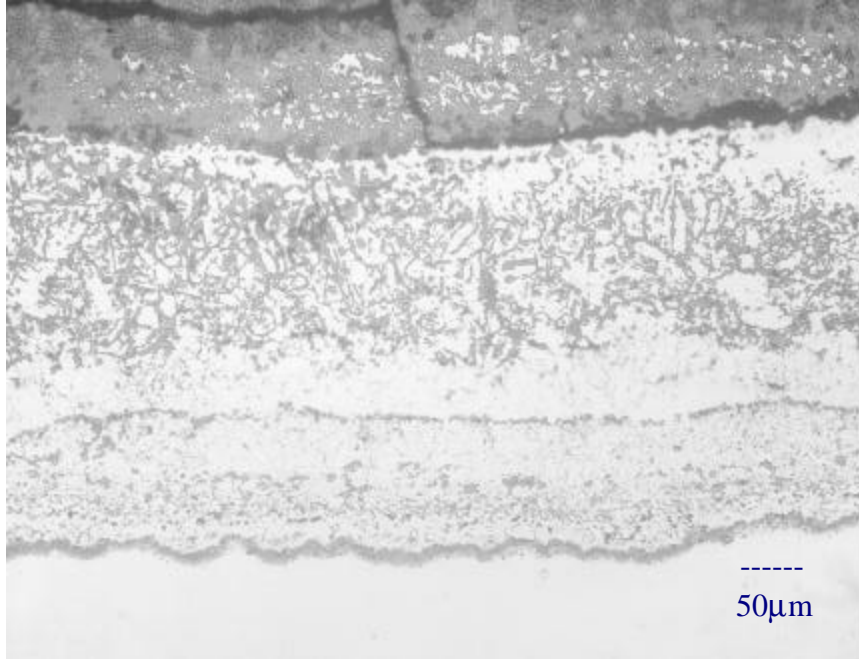


Figure 9. Photomicrograph showing cross section of alloy 690 sample after exposure for 336 hours in  $N_2$ -10% $O_2$ -10% $CO_2$ -20% $H_2O$ -1500ppm HCl-300ppm  $SO_2$  at 550°C. Sample was painted with ash 1. Unetched.

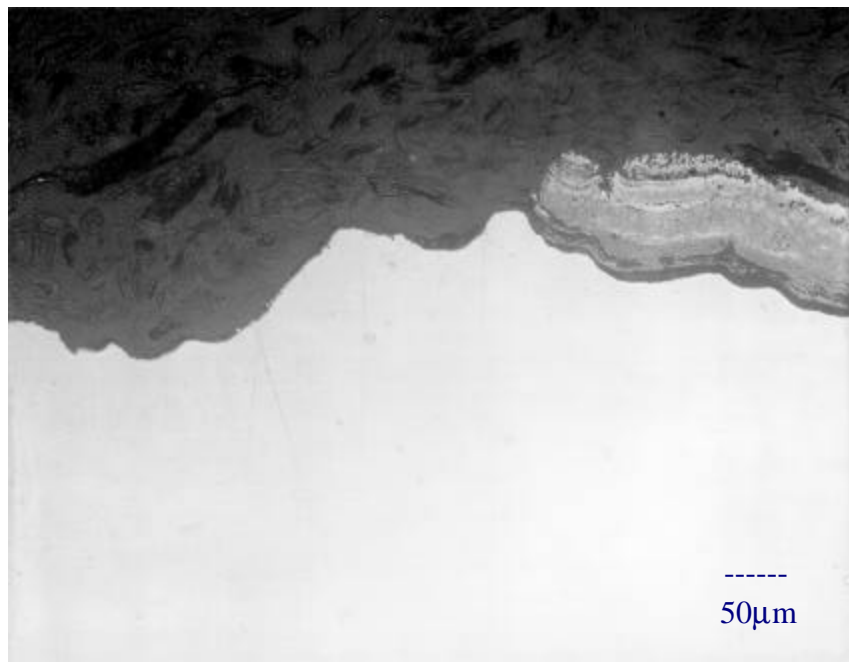


Figure 10. Photomicrograph showing cross section of alloy 825 sample after exposure for 336 hours in  $N_2$ -10% $O_2$ -10% $CO_2$ -20% $H_2O$ -1500ppm HCl-300ppm  $SO_2$  at 550°C. Sample was painted with ash 1. Unetched.



Figure 11. Photomicrograph showing cross section of alloy 686 sample after exposure for 336 hours in  $N_2$ -10% $O_2$ -10% $CO_2$ -20% $H_2O$ -1500ppm HCl-300ppm  $SO_2$  at 550°C. Sample was painted with ash 1. Unetched.

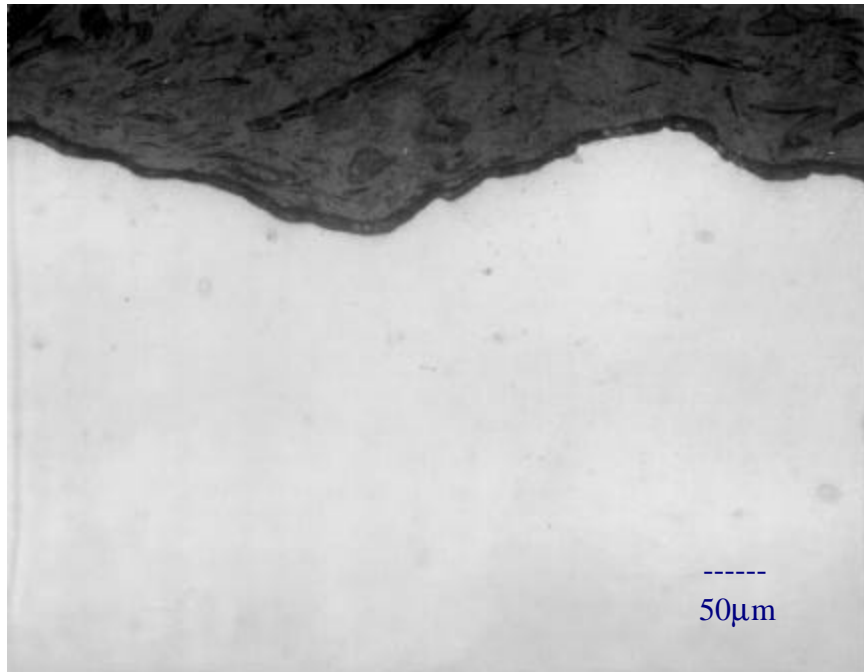


Figure 12. Photomicrograph showing cross section of alloy 625 sample after exposure for 336 hours in  $N_2$ -10% $O_2$ -10% $CO_2$ -20% $H_2O$ -1500ppm HCl-300ppm  $SO_2$  at 550°C. Sample was painted with ash 1. Unetched.

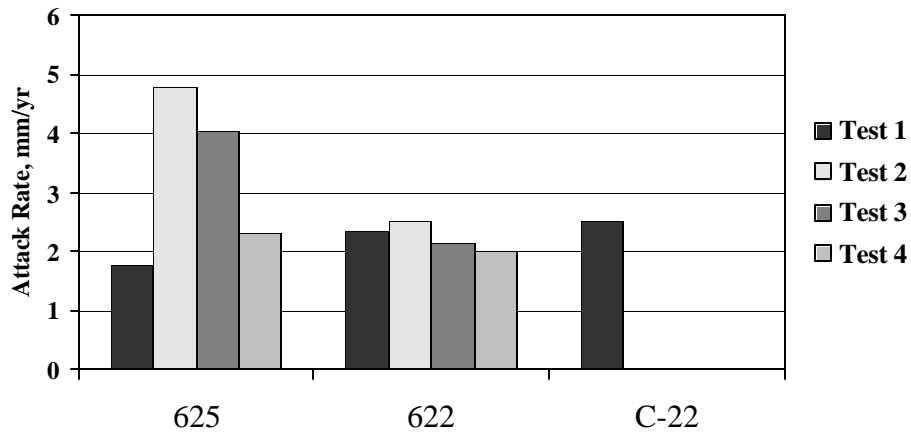


Figure 13. Corrosion Rate Measurements for Alloys 625, 622 and C-22 after Exposure for 336 Hours in  $N_2$ -10% $O_2$ -10% $CO_2$ -20% $H_2O$ -1500ppm HCl-300ppm  $SO_2$  at 550°C - Samples Painted with Ash 1.

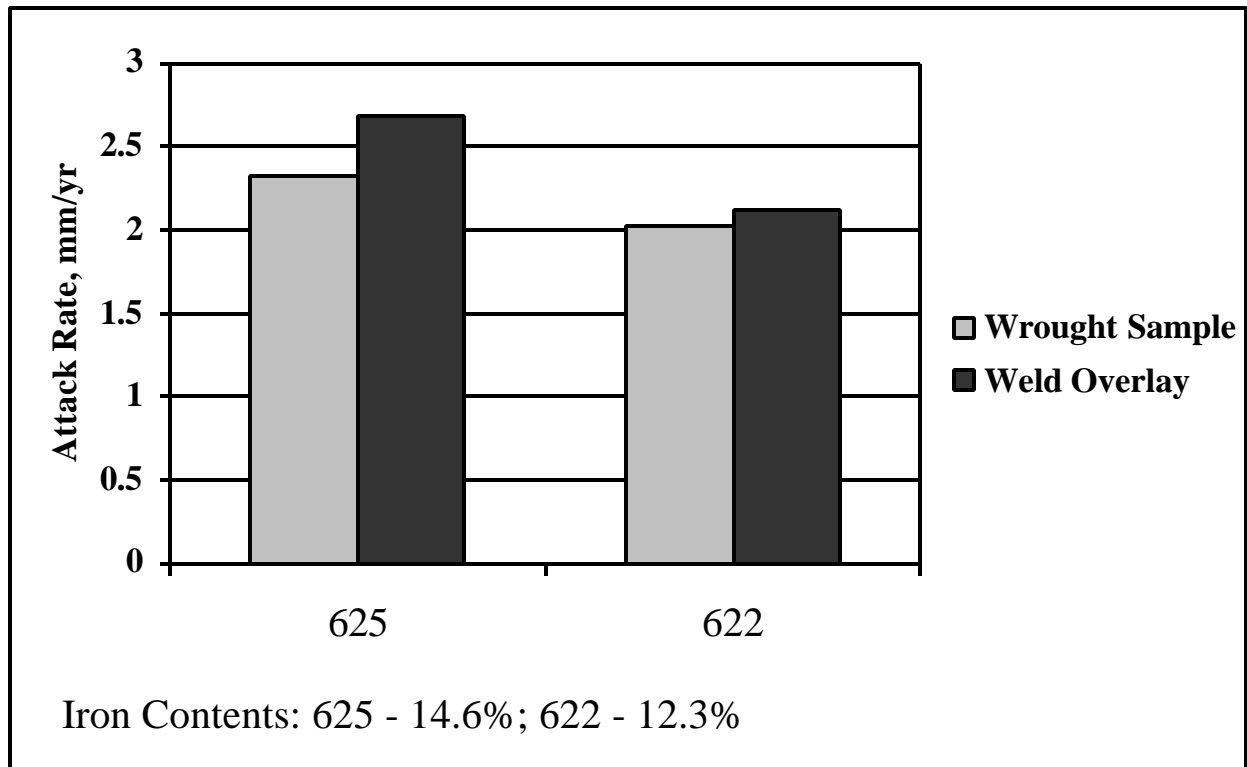


Figure 14. Corrosion rate measurements for alloys 625 and 622 after exposure for 336 hours in  $N_2$ -10% $O_2$ -10% $CO_2$ -20% $H_2O$ -1500ppm HCl-300 ppm  $SO_2$  at 550°C. Samples were painted with salt mixture 1.

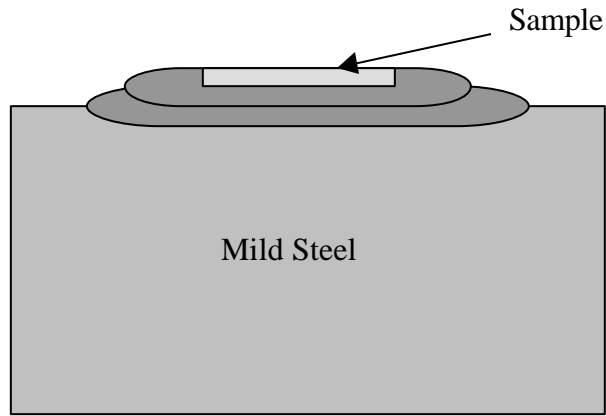


Figure 15. Drawing (not to scale) showing cross section of submerged-arc weld overlay and sample cross section. All sample surfaces machined and ground to 120-grit.

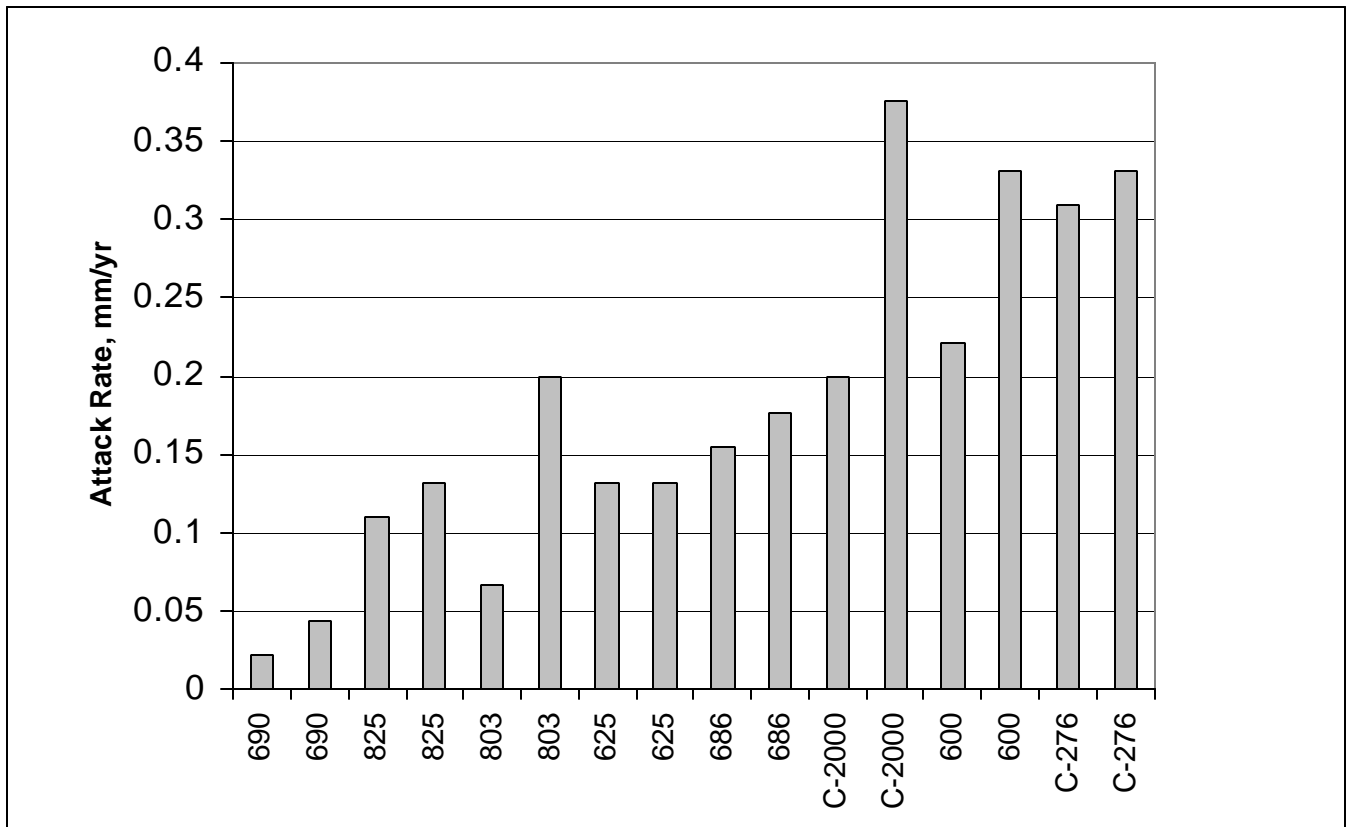


Figure 16. Attack rate measurements after exposure for 1008 hours in  $N_2$ -10% $O_2$ -10% $CO_2$ -20% $H_2O$ -1500ppm HCl-300 ppm  $SO_2$  at 550°C. Samples were painted with ash 2.